Dalton Transactions

An international journal of inorganic chemistry

Accepted Manuscript

This article can be cited before page numbers have been issued, to do this please use: J. Langwald, S. Burguera Piña, A. Frontera and M. S. Wickleder, *Dalton Trans.*, 2026, DOI: 10.1039/D6DT01115B.

ROYAL SOCIETY OF CHEMISTRY

rsc.li/dalton

Structural Insights Into Heavy Chalcogen Polycations and Their Stabilization via (Hydrogen)polysulfates.

View Article Online
DOI: 10.1039/D6DT01115B

Jan Langwald,[a] Sergi Burguera,[b] Antonio Frontera *[b] and Mathias S. Wickleder*[a]

[a] *Institute of Inorganic and Materials Chemistry, University of Cologne, Greinstr. 6, 50939 Cologne, Germany. E-mail: mathias.wickleder@uni-koeln.de*
[b] *Universitat de les Illes Balears, Crta de Valldemossa km 7.5, 07122 Palma de Mallorca, Baleares, Spain. E-mail: toni.frontera@uib.es*

Abstract

We report the preparation and characterization of the cations $[Se_4]^{2+}$, $[Te_4]^{2+}$ and $[Te_6]^{4+}$, stabilized as polysulfates, namely $[Se_4][S_2O_7]$, $[Se_4][HS_2O_7]_2$, $[Se_4][HS_3O_{10}]_2$, $[Te_4][HS_3O_{10}]_2$, $[Te_6][HS_3O_{10}]_4$ and $[Te_6][S_4O_{13}]_2$. In case of the tellurium compounds, this represents the first stabilization and solid-state investigations of the species from chlorosulfuric acid / sulfur trioxide-based media, although the respective colorful solutions are known for over 200 years. The unusual cation–anion interaction was investigated via Density functional theory (DFT) calculations, i.e. MEP surface plots, QTAIM and NBO analyses. The non-covalent interactions (chalcogen bonding (ChB)) within the novel species reveal different binding modes, namely bifurcated (Ch···O,O or Ch,Ch···O) as well as standard (Ch···O) σ-hole interactions. We show that the $[Se_4]^{2+}$ dication exhibits an electrophilic duality, engaging in σ- as well as π-hole interactions and that the stabilization of polycationic chalcogens with oxoanions is enhanced by auxiliary Ch···O contacts.

Introduction

The colorful solutions of tellurium and selenium in concentrated sulfuric acid are known for over 200 years,[1-2] and even nowadays they are still shown in every freshman lecture.[3-4] Remarkably, the study of these solutions began only in the late 1960s, led predominantly by *Gillespie* and his colleagues.[5-8] Although these first studies were restricted to spectroscopic and conductometric investigations, the authors were already able to distinguish different polycationic species and they made very accurate assumptions on the geometry of the respective species.[9-10] Notably, though several solids were isolated from these media and analyzed via classical quantitative elemental analysis or conductometry, the only crystallographically elucidated species was and remains until today, $[Se_4][HS_2O_7]_2$ (**1**).[11] In the following decades, the stabilization of chalcogen polycations switched from (hydrogen-)polysulfates towards halidometalates like $[AlCl_4]^-$ [12-13], $[PnF_6]^-$ (Pn = As, Sb)[12, 14-15] or $[MCl_6]^-$ (M = W, Zr, Hf)[16-17] (see Figure 1).[18] This is also true for many mixed chalcogen polycations like $[Te_2Se_n]^{2+}$ (n = 2, 4, 6, 8) [19-22] and the higher-condensed cations like $[Se_n]^{2+}$ (n = 8, 10)[23-25]. It was not until 2016, when *Beck* and coworkers were able to isolate the species $[Te_4]^{2+}$, $[Te_6]^{4+}$ and $[Te_8]^{6+}$ with oxoanionic, yet fluorinated, systems like $[F_3CSO_3]^-$ or $[C(SO_2CF_3)_3]^-$, using electrochemical synthesis.[26] Especially for tellurium, extensive reviews on the accessible (polycationic-) structures and the bonding behavior have been published by *Beck*, *Chivers* and *Laitinen*.[27-28]

While several assumptions for the species existing in solutions of tellurium and selenium in fluorosulfuric acid or oleum were made, e.g. $[Se_4][S_4O_{13}]$[5] or $[Te_4][HS_3O_{10}]_2$,[29] the isolation,

View Article Online
DOI: 10.1039/D6DT01115B

crystallographic proof and structural analysis of the species that are present in these systems remain an unsolved challenge. Their investigation is not only of academic interest to finally elucidate the possible equilibria between cations and anions in these superacidic media but might also bring additional insight for the research on Se/Te species as conductors or battery materials.[30-32]

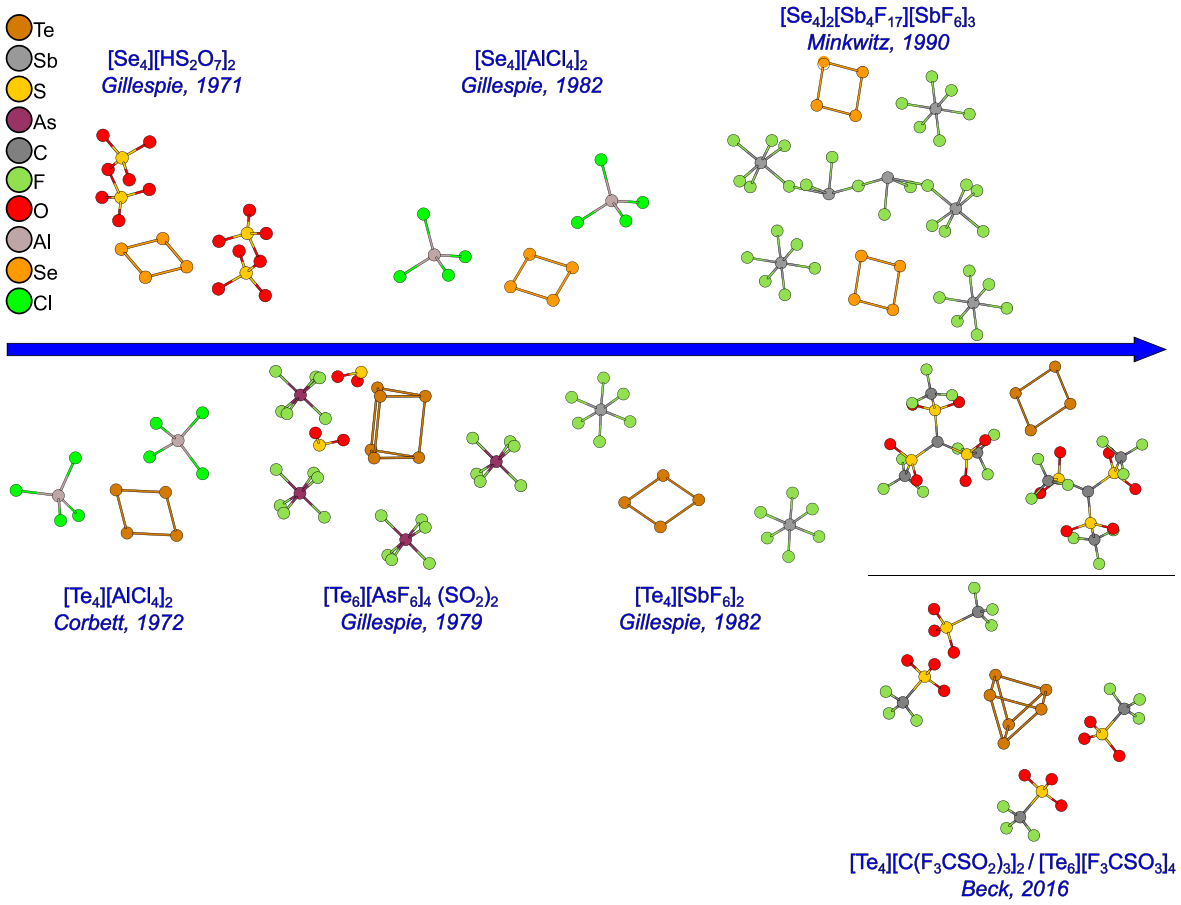

Figure 1: Timeline showing the crystallographically elucidated $[Se_4]^{2+}$, $[Te_4]^{2+}$ and $[Te_6]^{4+}$ systems using main-group based anions.[11-15, 26]

We were now able to isolate and structurally elucidate the neat disulfate $[Se_4][S_2O_7]$ (**2**) and the three novel (poly-)chalcogen hydrogentrisulfates $[Se_4][HS_3O_{10}]_2$ (**3**), $[Te_4][HS_3O_{10}]_2$ (**4**) and $[Te_6][HS_3O_{10}]_4$–I (**5**), the latter one also in a second modification $[Te_6][HS_3O_{10}]_4$–II(**6**). This is the first time that the cations $[Te_4]^{2+}$ and $[Te_6]^{4+}$ are stabilized in a purely oxoanionic environment and enables the direct comparison of both cations, as well as the lighter congener $[Se_4]^{2+}$, within the same anionic environment. Additionally, we re-determined the structure of the known compound **1**. We present single crystal X-ray diffraction (SCXRD) data at 100 K, to directly compare the differences between the other anions $[S_2O_7]^{2-}$ / $[HS_3O_{10}]^{2-}$ and derive potential trends for the stability of the respective systems. Finally, we also isolated the novel tetrasulfate $[Te_6][S_4O_{13}]_2$ (**7**), which helps to further understand the influence of different Lewis basic oxoanions on the same cation. Our analysis of the interactions within these systems show σ- and π-hole chalcogen bonding by the respective cations. Interest in non-covalent interactions, i.e. chalcogen bonding (ChB)[33-34], spans from crystal engineering[35-36] over catalysis,[37-38] to small molecule uptake, anion transport and supramolecular assembly.[39-42] Since these studies often focus on the interaction of 'organic' *Lewis* basic chalcogen bond acceptors, we wanted to

View Article Online
DOI: 10.1039/D6DT01115B

contribute to the better understanding of non-covalent interactions for the stabilization of unusual main-group (poly-)cations within 'inorganic' systems.

Results and Discussion

Syntheses

$[Se_4][HS_2O_7]_2$ (compound **1**) is readily available via solvothermal synthesis of elemental selenium with neat SO_3 in combination with a suitable proton donor, either $ClSO_3H$ or 1,2-dichloroethane, at 80°C in closed glass ampoules (detailed experimental information in the electronic supporting information [ESI]). The compound forms characteristic bright orange crystals and can be prepared phase pure (verified via PXRD, see ESI, Fig. S 2). If a mixture of Se, $ClSO_3H$ and SO_3 (in excess) is stored at -20 °C for 3 weeks, bright yellow crystals grow, which were identified as the hydrogentrisulfate $[Se_4][HS_3O_{10}]_2$ (**3**).

Compound **3** decomposes, if not stored in an SO_3-rich atmosphere, also in an Ar-glovebox, and transforms into the thermodynamically more stable hydrogendisulfate **1** with release of SO_3, visible by color change from bright yellow to orange. This also occurs upon grinding (see ESI, Fig. S 9), preventing phase pure powder preparation of compound **3** (see ESI, Fig. S 10). Both compounds can be discriminated by their Raman spectra, which differ in the amount and intensity of their S–O vibrational modes (see ESI, Fig. S 26). Formation of the neat disulfate $[Se_4][S_2O_7]$ (**2**) is more challenging, since the bright yellow $[Se_4][S_4O_{13}]$ always forms when neat selenium, SeO_2 or $SeOCl_2$ are reacted with SO_3 at elevated temperatures.[43] We were able to isolate compound $[Se_4][S_2O_7]$ as a byproduct from the reaction of elemental bismuth with selenoyl chloride and SO_3.[44] As for the hydrogendisulfate, the disulfate crystallizes as bright orange blocks. Attempts to differentiate between the formation of several species using ^{77}Se NMR experiments (in $ClSO_3H$ / D_2CCl_2) showed no signals within the range +2100 ppm – -50 ppm. Direct preparation of solutions, e.g. of **1**, in usual solvents was not possible, in line with the findings of *Gillespie*.[7] Solutions of elemental Se in $ClSO_3H$ / D_2CCl_2 are initially dark green, indicating the formation of the $[Se_8]^{2+}$ cation, but transform into yellow within a period of 24 h at r.t. and ~ 3 weeks at -20 °C.[45]

The Te compounds **4**–**6** can be isolated as single crystals directly from a mixture of Te, $ClSO_3H$ and SO_3 at 7 °C and are distinguishable by their color, $[Te_4]^{2+}$ being red and $[Te_6]^{4+}$ being colorless to slightly yellow, in accordance to the observations of *Gillespie*.[46] $[Te_4][HS_3O_{10}]_2$ (**4**) and $[Te_6][HS_3O_{10}]_4$–I/–II (**5**) + (**6**), all being colorless, can only be distinguished by very small differences in the crystal habit. They are readily oxidized towards $Te[S_2O_7]_2$ upon heating to 80°C.[47] Overoxidation by SO_3 can be partially prevented by using the system Te, $SOCl_2$ and SO_3, i.e. working with a 'solvent', which leads to formation of $[Te_6][S_4O_{13}]_2$ (**7**) as pale yellow crystals, besides colorless $Te[S_2O_7]_2$. If lower temperatures are applied, no suitable crystal growth can be realized. The use of $SOCl_2$ as a solvent or cooling of the reaction does not fully inhibit the total oxidation towards $Te[S_2O_7]_2$, making a phase pure preparation of the tellurium species challenging so far. Due to this, spectroscopic characterization of the respective species was not achieved yet. Nonetheless, all compounds can be reproducibly made and we could identify all species several times using SCXRD.

View Article Online
DOI: 10.1039/D6DT01115B

Solid-state Structures

The bond lengths between the chalcogen atoms (Ch) within the cations are in very good agreement to the reported literature values (see Figure 2).[48-49] The $[Se_4]^{2+}$ cations in **1**, **2** and **3** are slightly, but not significantly different. They all show almost D_{4h} symmetry, even if the symmetries in the solids are only C_i (**1** and **3**) and C_1 (**2**), respectively. Thus, for **1** and **3** two different Se-Se distances are found while four different values occur for the cation in **2**. In any case, the distances are in a very narrow range with a mean value of 228,6 pm (see also ESI). Obviously, the distances within the $[Se_4]^{2+}$ cation are essentially independent from the nature of the counter anion. This finding is different from the observations for the $[I_4]^{2+}$ cation, which shows remarkable bond lengths alteration with respect to the stabilizing anions.[50] The reason for this observation is that the $[Se_4]^{2+}$ is a 6π-aromatic system while in the rectangular $[I_4]^{2+}$ ions two $[I_2]^{+}$ cations are linked only by a weak bond. Accordingly, for the $[Te_4]^{2+}$ cation, which is also a 6π-aromatic system, the observed Te-Te distances in **4** are almost identical to the compounds reported so far. This is significantly different for the non-aromatic trigonal prismatic $[Te_6]^{4+}$ cation. It consists of two $[Te_3]$ triangles with short Te-Te distances, comparable to those found for the $[Te_4]^{2+}$ ion, combined by longer Te-Te bonds linking the triangles to the trigonal prism. Especially these longer bonds seem to be very sensitive to the nature of the surrounding anions (Fig. 2).

Anion	Se–Se	Te–Te	Te–Te / Te–Te'
	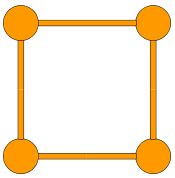	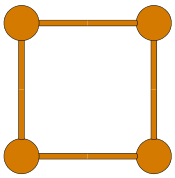	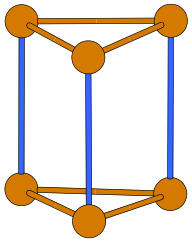
$[S_2O_7]^{2-}$	228.09(3) – 229.04(3)	/	/
$[HS_2O_7]^{-}$	228.37(4) – 228.80(3)	/	/
$[HS_3O_{10}]^{-}$	228.44(6) – 228.80(6)	266.68(4) – 266.98(4)	268.72(8) – 271.46(7) 306.51(8) – 324.30(8)
$[S_4O_{13}]^{2-}$	228.53(7) – 229.18(6)	/	268.91(8) – 271.35(6) 311.90(6) – 314.71(8)
$[AlCl_4]^{-}$	228.3(2)	266.3(2) – 267.4(2)	/
$[AsF_6]^{-}$	/	/	266.2(3) – 267.3(2) 306.2(2) – 313.2(2)
$[F_3CSO_3]^{-}$ $[C(F_3CSO_3)_3]^{-}$	/	266.71(3) – 267.03(3)	269.22(4) – 272.35(6) 306.09(3) – 313.46(5)
calculated	228.0 – 228.6	266.3 – 267.4	/

Figure 2: Ch–Ch bond lengths (in pm) within the $[Se_4]^{2+}$, $[Te_4]^{2+}$ and $[Te_6]^{4+}$ cations in the novel compounds, the literature-known compounds with $[S_4O_{13}]^{2-}$[43], $[AlCl_4]^{-}$[12-13],$[AsF_6]^{-}$[15], $[F_3CSO_3]^{-}$[26] and calculated values[48].

View Article Online
DOI: 10.1039/D6DT01115B

Another interesting feature of the presented compounds are polysulfate anions. Especially the $[HS_3O_{10}]^-$ anion has been rarely described in literature. The bond lengths in the $[HS_2O_7]^-$ anion of the low-temperature modification of **1** (see ESI, Table S4) are in good agreement with the 293 K data reported by *Gillespie*. The slight deviations in the terminal S–O bond lengths and the Se···O distances can be attributed to the different measuring temperature and an increased accuracy of the used diffractometer.[11] The structure shows hydrogen bonding between the O13 (S–OH) atom of one $[HS_2O_7]^-$ unit and the O22 (terminal) oxygen atom of a second $[HS_2O_7]^-$ unit (see ESI, Fig. S4). The H···O and O···O distances of 183.1(5) pm and 258.3(2) pm, as well as the O–H–O angle of 167° indicate a moderate hydrogen bond, according to *Steiner*.[51] While the terminal, non-coordinating bonds S–O_t, the bridging bonds S–O_{br} and the S–OH bonds show distances in good agreement with the literature known hydrogendisulfates [M][HS_2O_7] (M = K, Cs, Rb, [NH_4], [NO])[52], the terminal coordinating S–O_t bond lengths are elongated (~1 pm) for compound **1**, which indicates slightly increased cation···anion interaction. If the S–O bond lengths within $[Se_4][HS_2O_7]_2$ are compared to the disulfate $[Se_4][S_2O_7]$ and the hydrogentrisulfate $[Se_4][HS_3O_{10}]_2$, significant differences become apparent (see Figure 3). The increased asymmetry of the S–O–S bridges, which is known for polysulfate systems and can be explained by the polysulfate chain growth via *Lewis* adduct formation [53], can be observed for the hydrogenpolysulfates as well, when comparing the bond lengths of the anions in **1** and **3**. Additionally, a pronounced differentiation between the terminal, non-coordinating (S–O_t) and coordinating (S–O_{co}) bonds can be observed.

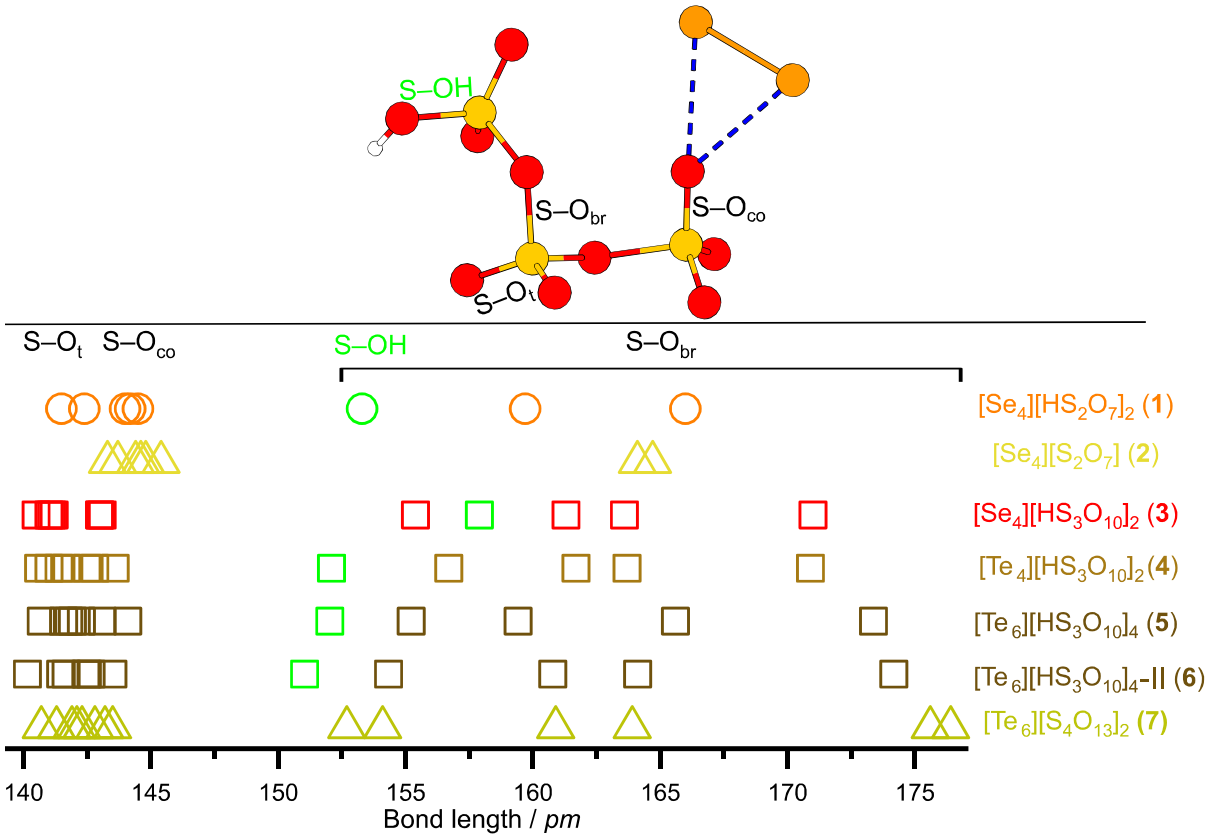

Figure 3: Bond lengths within the anions of compounds **1**–**7** given in pm. t = terminal, co = coordinating, br = bridging.

View Article Online
DOI: 10.1039/D6DT01115B

Usually, the S–O_{co} bond length decreases with increasing (hydrogen-)polysulfate chain length for the same cation due to decreased Lewis basicity of the anion. This can be seen when comparing the elongated S–O_{co} bond lengths of the stronger Lewis basic disulfate $[S_2O_7]^{2-}$ (**2**), with the slightly shorter ones of the hydrogendisulfate $[HS_2O_7]^-$ (**1**). When increasing the chain length of the (hydrogen-)polysulfate anion, its Lewis basicity further decreases, which can be seen when comparing the hydrogendi- and trisulfate (**1** and **3**).

Nonetheless, the respective bonds within **3** are still elongated by 1–2 pm when compared to the alkaline metal hydrogentrisulfates.[54] The most notable difference for compound **3** is the starkly increased S–OH bond length for the hydrogentrisulfate. With a value of 157.9(4) pm, it is roughly 5 pm longer compared to the findings for **1** and the tellurium hydrogentrisulfates **4**–**6**, and up to 9 pm longer compared to the group I hydrogentrisulfates. The hydrogen bonding between the anions in **3** is stronger compared to **1** (H···O = 172.9(3) pm, O···O = 255.8(5) pm, O–H–O = 169°; see ESI, Fig. S 12). However, this is no suitable explanation for the increased S–OH bond length, since the hydrogen bonding within the anions of the related tellurium species **4** is comparably strong (H···O = 169.3(7) pm, O···O = 253.1(5) pm, O–H–O = 163°; see SI, Fig. S 15), but the respective S–OH bond within $[Te_4][HS_3O_{10}]_2$ is 152.1(3) pm long and thus aligns perfectly with the other hydrogentrisulfate species reported so far ($[M][HS_3O_{10}]$ (M = Na, K, Rb)[54]) and herein. The S–O bond lengths within compound **7** are in good agreement with the observations for $Li_2[S_4O_{13}]$[53] and $Ba[S_4O_{13}]$[55] (see ESI, Table S 49), highlighting the strong Lewis acidity of $[Te_6]^{4+}$, albeit being a cluster cation with a formal charge of +2/3 per Te atom.

The lability of compound **3** towards release of SO_3 can be explained with the increased terminal bridging S–O–S bond length. For longer-chained (hydrogen-)polysulfates, we introduced the δ-value as an additional parameter to characterize the strength of the terminally bound SO_3 unit and to estimate the adduct character of a polysulfate.[53] The δ-values of compounds **1** and **2** are unexpectedly high (see ESI, Table S. 50 and Fig. S. 25), comparable to values found for the disulfate of the highly Lewis acidic $[ICl_2]^+$ cation.[53] Since the respective O···Se distances are comparable to the O···I distances in $[ICl_2]_2[S_2O_7]$, but the van der Waals volume of selenium is significantly smaller than for iodine, this already indicates that different coordination motifs are present for the $[Ch_4]^{2+}$ species. The δ-values of compounds **3** and **4** are decreased compared to the group I hydrogentrisulfates, meaning that the terminal SO_3 units have no strong degree of pyramidalization and are weakly bound. The δ-values nonetheless align nicely with the general trend visible for other reported $[HS_3O_{10}]^-$ compounds. In general, the elongated S–O_{br} bond as well as the decreased δ-value indicate weak donor-acceptor (DA) interactions between the anion and the cation. However, within the novel compounds, strong non-covalent interactions (σ- and π-hole chalcogen bonding) are observed. The DA distances within the novel compounds are shown in Figure 4.

Compound **1** shows the shortest O···Se distance within all compounds (267.6(2) pm), although the DA distances are more widely distributed than for compound **2**, which displays O···Se distances between 268.5(2) pm and 280.7(2) pm, as well as for compound **3**, showing narrowly distributed DA distances between 270.0(3) pm and 271.2(3) pm. An increase in the DA distance is usually expected for decreasing Lewis basicity when moving from $[HS_2O_7]^-$ towards $[HS_3O_{10}]^-$ anions. However, the planarity of the cation–anion coordination is greatly increased

View Article Online
DOI: 10.1039/D6DT01115B

for the latter, which in turn indicates a stronger DA interaction. The high planarity is also found for the heavier chalcogen polycation $[Te_4]^{2+}$.

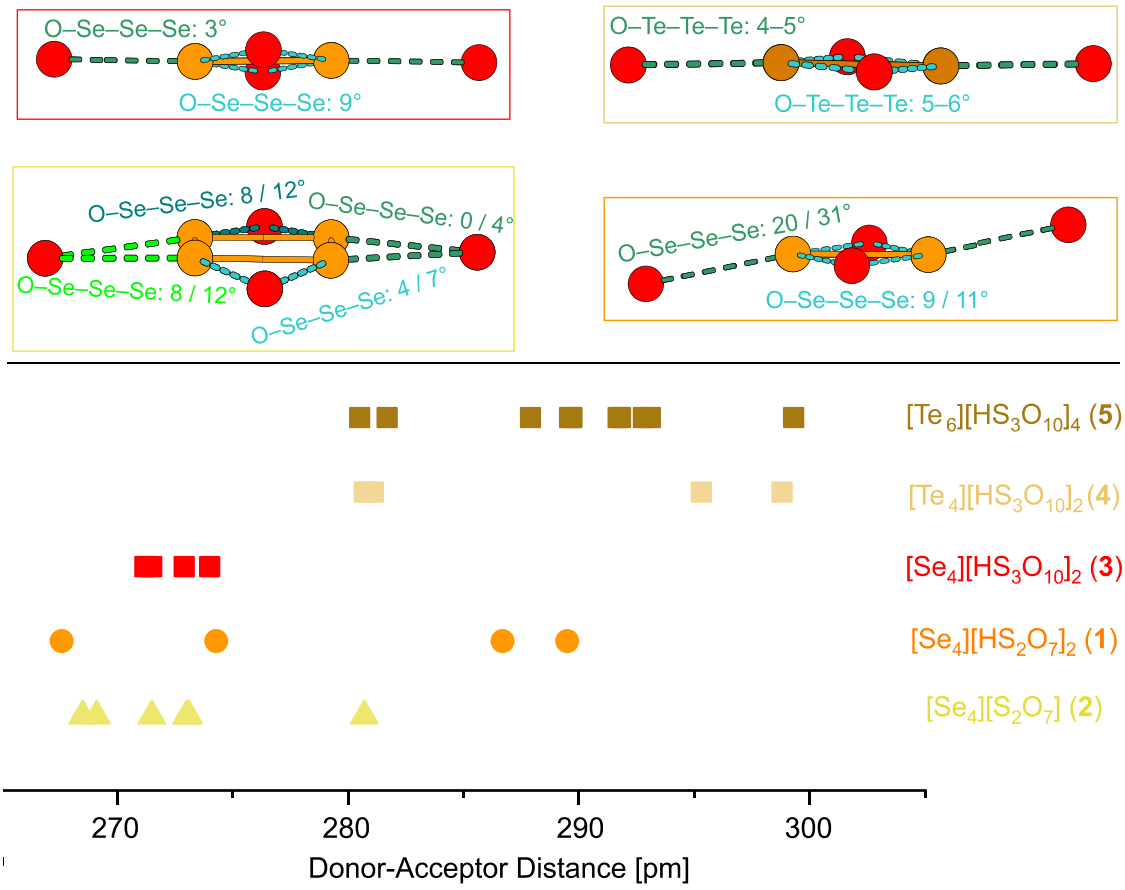

Figure 4: Donor-Acceptor Distances (O···Ch [Ch = Se, Te]) for compounds **1**–**5** in pm. The O–Ch coordination within the $[Ch_4]^{2+}$ plane for **1**–**3** and the O–Ch–Ch–Ch torsion angles are shown above the graph.

All $[Ch_4]^{2+}$ species show a 'star-shaped' coordination pattern of the closest coordinating oxoanions, already known from compound **1**, which is in good agreement to reported $[Ch_4]^{2+}$ species with other Lewis basic coordination sites, e.g. $[Ch_4][AlCl_4]_2$ (Ch = Se, Te)[12-13] or different polynitriles (di-/tetracyanobenzenes)[56]. Notably, the terminal SO_3 unit of the hydrogenpolysulfate anions within compounds **1**, **3** and **4** is coordinatively saturated, with two oxygen atoms being involved in chalcogen bonding while the remaining oxygen atom is part of the hydrogen bond between the anions, forming 2–D chains along the crystallographic b-axis within the $[Ch_4]^{2+}$ compounds (see ESI, Fig. S 4, 12 and 15), and dimers in case of the $[Te_6]^{4+}$ compounds (see ESI Fig. S 18). Since all hydrogentrisulfate species reported herein are prone to overoxidation if elevated temperatures are applied and the respective crystals were isolated at reduced temperatures (7°C and –20°C, respectively), we attribute their stabilization to the extensive additional lattice stabilization energy via hydrogen bonding.

For the $[Te_6]^{4+}$ species within compounds **5**–**7**, the O···Te coordination environment differs compares to the $[Se_4]^{2+}$ species. Due to its non-aromaticity, the cation-anion interactions show increased directionality and the unusual behavior of bi- and even tridentate coordination of a (hydrogen-)polysulfate anion (see ESI, Fig. S 17, S 20 and S22).

View Article Online
DOI: 10.1039/D6DT01115B

Although bidentate, directional coordination was proposed from DFT calculations for the system $[Te_4][OAc]_2$[57], it is not found experimentally within the $[Te_4]^{2+}$ species discussed here. The respective Te–Te bond lengths within the $[Te_6]^{4+}$ ions are slightly elongated compared to the $[AsF_6]^-$ system but in excellent agreement to the $[F_3CSO_3]^-$ salt.[15, 26] The $[Te_6]^{4+}$ unit within compound **7** is generated due to symmetry, since the atoms Te2 and Te3 are situated on a mirror plane (Wyckoff site 4*c* of space group *Pnma*). Thus, the asymmetric unit (ASU) does not show the complete prismatic $[Te_6]^{4+}$ ion but a pseudo '$[Te_4]^{2+}$' rectangle (see ESI, Fig. S 21). Accordingly, the Te–Te bonds within **7** are highly symmetric and the resulting prism is differing from the compounds **4** and **5**, which show the literature known boat conformation.[58-59] The only other example with similar regular symmetry is $[Te_6][AsF_6]_4{\cdot}2SO_2$[15], while the irregular, one- or two-side elongated prism is more commonly found in both homo- and heteroatomic chalcogen polycations.[60-61] This is a notable difference from the DFT calculations performed on these species, where the elongated-prismatic structure or the boat structure are predicted to be energetically more stable.[62]

The coordination of the oxoanions towards the $[Ch_4]^{2+}$ and $[Te_6]^{4+}$ species seems to slightly deviate from 'classical' σ-hole interaction, since the O···Ch (Ch = Se, Te) coordination is found towards the center of the Ch–Ch bonds, rather than towards the bond extension. In turn, other planar units, e.g. the S_2O_2 and $[S–C]_2$ unit within 2,2,4,4-tetrafluoro-1,3-dithietane, show large π-character of the bonds and the observed electron density indicate that π-hole interactions might be energetically favored over classical σ-hole interactions in these and related systems.[63] Since, to our knowledge, no extensive quantum chemical analysis on the coordination behavior and bonding of $[Ch_4]^{2+}$ and $[Te_6]^{4+}$ was reported so far, we sought to analyze the herein observed interactions in more detail.

Quantum Chemical Calculations

The solid-state structures of compounds **1**-**7** exhibit multiple Se···O and Te···O contacts, respectively, that are formally classified as chalcogen bonds (ChB). Given the ionic nature of the compounds, the overall crystal packing is primarily established by strong bulk electrostatic (Coulombic) effects. However, while these long-range interactions dominate the assembly's energy profile, the final supramolecular architecture is precisely fine-tuned by the specific directionality inherent to the σ-hole interaction. This arises directly from the anisotropy of the charge distribution around the covalently bonded chalcogen atom, where a localized region of positive electrostatic potential (the σ-hole) selectively attracts the nucleophilic oxygen acceptor. To investigate the most electrophilic regions in the cationic fragments $[Se_4]^{2+}$, $[Te_4]^{2+}$, and $[Te_6]^{4+}$, we calculated their *Molecular Electrostatic Potential* (MEP) surfaces, which are presented in Figure 5.

View Article Online
DOI: 10.1039/D6DT01115B

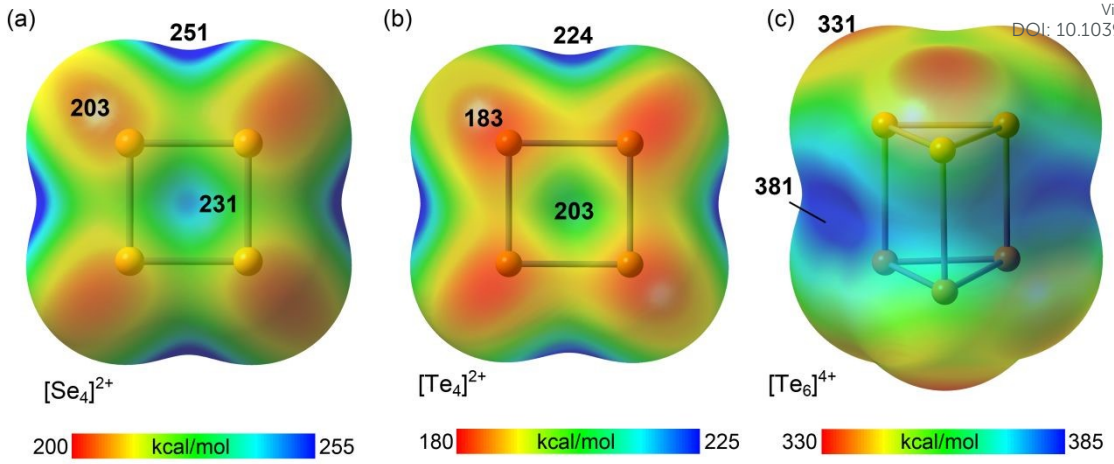

Figure 5: Molecular Electrostatic Potential (MEP) Surfaces of the Cationic Fragments. MEP surfaces mapped onto the 0.001 a.u. electron density isosurface for the (a) $[Se_4]^{2+}$ and (b) $[Te_4]^{2+}$ dications, and (c) $[Te]_6^{4+}$ tetracation. Color scales for the MEP surfaces are shown below each structure, where blue indicates the regions of maximum positive potential (electrophilic sites) and red indicate less-positive regions.

For the square dications, $[Se_4]^{2+}$ (a) and $[Te_4]^{2+}$ (b), the σ-holes, corresponding to the maximum positive electrostatic potential ($V_{S,max}$), are located at the center of each side, along the extension of the Ch-Ch bond. This position of the σ-holes slightly deviates from the highly directional σ-holes usually found in the extension of a bond as known from halogen-,[53, 64] chalcogen-, and pnictogen bonding within organic compounds.[65] It aligns with a trend which we already analyzed for ChBs within sp^3 and sp^2 hybridized Se or Te species with nitrogen Lewis bases and explains the observed coordination behavior in the solid-state structures.[66] The deviation of the expected positions of positive MEP and coordination of the oxoanions towards the σ-holes strongly underline the arguments of *Politzer*, that maxima identified *via* V_S are local maxima and that an increasing non-linearity due to polarization and the influence of secondary interactions can be observed for the non-covalent interactions of group VI atoms in the solid state, compared to isolated gas-phase calculations.[67-69]

Intriguingly, $V_{S,max}$ of $[Se_4]^{2+}$ (251 kcal/mol) is more positive than that of the heavier congener, $[Te_4]^{2+}$ (224 kcal/mol). This finding is contrary to the general trend observed in divalent chalcogen derivatives, where the σ-hole potential typically increases with the polarizability (atomic size) of the chalcogen atom. Additionally, a π-hole is observed over the center of the square ring, with a potential of 231 kcal/mol for $[Se_4]^{2+}$ and 203 kcal/mol for $[Te_4]^{2+}$. The significantly more intense π-hole in Se_4^{2+} aligns with experimental data showing the formation of π-hole-mediated ChBs only in the selenium derivative (see ESI, Fig. S 28) and explains the decreased planarity of the coordination plane of compound **1** mentioned before.

In the trigonal prismatic $[Te_6]^{4+}$ cation (c), the MEP values are, as expected for the higher charge density (4+), considerably more positive. The absolute maximum potential ($V_{S,max}$ = 381 kcal/mol) is localized at the center of the square faces of the trigonal prism. Conversely, the minima potential regions are situated over the atoms in the vertices of the triangular faces. We further analyzed the supramolecular assemblies by characterizing the Ch···O chalcogen bonds using the *Quantum Theory of Atoms-In-Molecules* (QTAIM) and the *Non-Covalent Interaction* (NCI) plot analysis (see ESI, Section F, Fig. S 27). We were able to

View Article Online
DOI: 10.1039/D6DT01115B

identify three different primary binding modes, whereby the bifurcated Ch···O,O ChBs are the strongest, as confirmed by the reduced density gradient (RDG) isosurfaces. This bifurcation further explains the deviating directionality. Additional 'auxiliary Ch···O contacts' (coordination by oxygen atoms within the polysulfate chain, which usually have decreased oxoanionic character) can be found for the hydrogentrisulfates and highlights the potential of these anions for the stabilization of polycationic species bearing different σ- or σ- and π-holes. Subsequently, we analyzed the ChBs in compounds **1**–**5** and **7** from an orbital perspective, focusing on the orbital donor-acceptor charge transfer (see Figure 6).

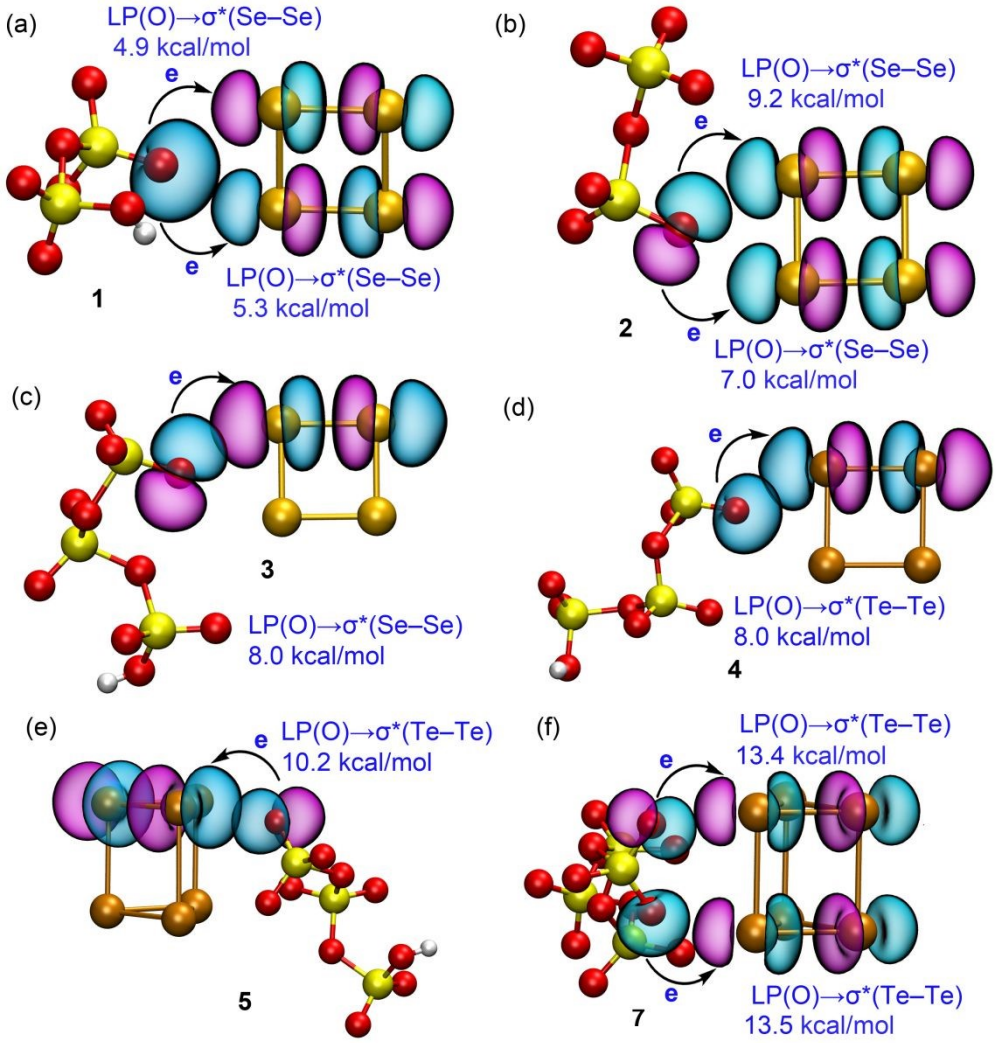

Figure 6: NBO plots illustrating the key stabilizing charge transfer interactions in compounds **1** (a), **2** (b), **3** (c), **4** (d), **5** (e), **7** (e). In all cases, the interaction is characterized by electron donation from the LP orbital of the nucleophilic O-atom into the antibonding σ* orbital of the chalcogen-chalcogen bond. The second order stabilization energies are indicated.

The main orbital contributions consistently show electron donation from the lone pair (LP) orbitals located on the terminal oxygen atoms of the (hydrogen-)polysulfate anions to the Ch–Ch antibonding σ* orbitals of the cations. These charge transfer energies range significantly, from 4.9 to 13.5 kcal/mol, thus quantitatively confirming the strong orbital effects inherent in these ChBs. It is particularly remarkable that the dominant bifurcated Se,Se···O ChB in compound **1** (Fig. 6a) results in two almost symmetric electron donations and stabilization

View Article Online
DOI: 10.1039/D6DT01115B

energies (4.9 and 5.3 kcal/mol) to the two opposite σ*(Se–Se) bonds of the $[Se_4]^{2+}$ square. While not fully depicted for simplicity, additional LP(O)→σ*(Ch–Ch) donations are also observed in all other bifurcated bonds, though these are increasingly asymmetric. The universal observation of the LP(O)→σ*(Ch–Ch) donation across all Ch···O contacts, combined with the significant stabilization energies, provide the underlying electronic rationale for the observed coordination motifs that dictate the solid-state architecture of compounds **1**–**7**. The symmetric electron donation of the oxoanions into the σ-holes of two chalcogen atoms also explains the deviating coordination geometry.

Lastly, we calculated the Frontier Molecular Orbitals (FMOs) of the $[Ch_4]^{2+}$ and $[Te_6]^{4+}$ units to analyze whether the differences observed in $V_{S,max}$ and the coordination behavior can be directly related to the respective HOMOs and LUMOs (see Figure 7).

The increased electrophilicity of the $[Se_4]^{2+}$ unit can be explained with the decreased energy of the LUMO. While the LUMO is basically identical for both $[Ch_4]^{2+}$ cations regarding the AO contributions, the HOMOs are notably different, whereby $[Te_4]^{2+}$ shows some biradical character. The existence of biradicaloid molecular orbitals within the $[Ch_4]^{2+}$ units was only described in the literature concerning the existence of degenerate, non-bonding orbitals.[49, 70] The biradicaloid character was reported to increase within the row S<Se<Te.[71] *Passmore* denoted that the structural chemistry and bonding within $[Te_4]^{2+}$ is more diverse compared to the lighter chalcogens due to different molecular orbital contributions.[72] The 6π aromatic square is predominantly formed with 'monomeric', hard counterions as $[PnF_6]^-$, while the formation of dimeric $[Te_8]^{4+}$ or polymeric $[Te_4]^{2+}_n$ species was reported for 'polymeric', higher charged anions like $[VOCl_4]^{2-}_n$.[60, 73-74] The di-/polymeric species built one-dimensional chains or two-dimensional folded bands and show Te–Te connectivity which can be directly correlated to the diradicaloid character. We propose that our novel compound **4** shows the unique transitions state between these two states.

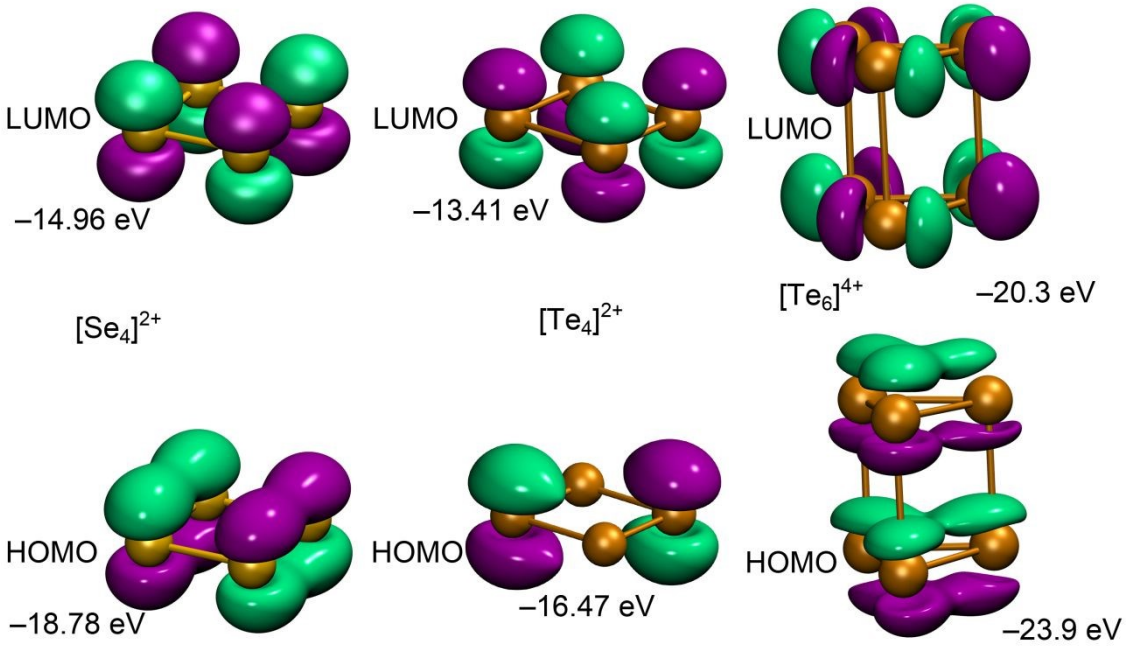

Figure 7: Frontier Molecular Orbitals (FMOs) for the isolated $[Ch_4]^{2+}$ and $[Te_6]^{4+}$ units and their respective energies in eV.

View Article Online
DOI: 10.1039/D4DT01115B

Although being a classical monomeric 6π aromatic $[Te_4]^{2+}$ unit with a square-planar geometry, it already shows the biradicaloid HOMO character. This also highlights that the bonding character of the cation can be gradually influenced via the anion. This is where our systems stand out due to their ability of forming 'auxiliary' donor-acceptor contacts due to the terminal oxygen atoms of the polysulfate chain.

Conclusion

In summary, we reported the isolation and structural characterization of the novel disulfate salt $[Se_4][S_2O_7]$ (**2**), the hydrogentrisulfate salts $[Se_4][HS_3O_{10}]_2$ (**3**), $[Te_4][HS_3O_{10}]_2$ (**4**), $[Te_6][HS_3O_{10}]_4$ (**5**) and $[Te_6][HS_3O_{10}]_4$–II (**6**) and the tetrasulfate salt $[Te_6][S_4O_{13}]_2$ (**7**), as well as the re-investigation of the hydrogendisulfate $[Se_4][HS_2O_7]_2$ (**1**). We presented an extensive structural analysis, highlighting the unusual coordination motifs between the oxoanions and the $[Ch_4]^{2+}$ cations, their differing donor-acceptor distances and the formation of supramolecular aggregates. The comprehensive computational analysis, combining MEP surfaces, QTAIM/NCIplot, and NBO analysis, provided compelling electronic evidence confirming that while the crystal packing of compounds **1**–**7** is globally governed by strong ionic (coulombic) forces, the final, high-resolution supramolecular architecture is dictated by the directionality of the ChBs through σ-hole interaction. The QTAIM and NCIplot analyses quantified these interactions, revealing strong (-6.1 to -9.4 kcal/mol) stabilization energies for the primary bifurcated binding modes. Our results indicate an electrophilic duality of the $[Se_4]^{2+}$, capable of engaging not only in robust σ-hole interactions but also in a secondary π-hole binding mode confirmed by LP(O) → π*(Se–Se) donation, showing the complex coordination sites of heavy chalcogen polycations. We could show that the stabilization of these species can be achieved by (hydrogen-)polysulfates as weakly coordinating anions, which not only show significant primary LP(O) → σ* charge transfer stabilization energies ranging up to 10.2 kcal/mol but are also able to develop secondary, auxiliary Ch···O contacts via the terminal oxygen atoms within the polysulfate chain.

Acknowledgements

The authors would like to thank Silke Kremer for the SCXRD measurements, Katrin Eppers and Arthur Edelmann for the Raman measurements and Daniel Moog for the P-XRD measurements. J.L. thanks Thomas Kasperowicz for helpful discussions and assistance with the Rietveld refinement. J.L. is thankful to the German National Scholarship Foundation (Studienstiftung des deutschen Volkes) for financial support.

Keywords: Polycations, (Pi interactions), Superacidic systems, Noncovalent interactions, Chalcogen bonding, Polysulfates

View Article Online
DOI: 10.1039/D6DT01115B

TOC graphic:

References

[1] Klaproth, *The Philosophical Magazine* **1798**, *1*, 78-82.
[2] G. Magnus, *Ann. Phys.* **1828**, *90*, 328-328.
[3] J. Strähle, E. Schweda, *Jander · Blasius Lehrbuch der analytischen und präparativen anorganischen Chemie*, 16 ed., S. Hirzel Verlag, Stuttgart, **2006**.
[4] N. Wiberg, *Holleman · Wiberg Lehrbuch der Anorganischen Chemie*, 102 ed., Walter de Gruyter, Berlin, **2007**.
[5] J. Barr, D. B. Crump, R. J. Gillespie, R. Kapoor, P. K. Ummat, *Can. J. Chem.* **1968**, *46*, 3607-3609.
[6] J. Barr, R. J. Gillespie, R. Kapoor, G. Pez, *J. Am. Chem. Soc.* **1968**, *90*, 6855-6856.
[7] R. J. Gillespie, G. P. Pez, *Inorg. Chem.* **1969**, *8*, 1229-1233.
[8] R. J. Gillespie, J. Passmore, *Acc. Chem. Res.* **1971**, *4*, 413-419.
[9] N. J. Bjerrum, G. P. Smith, *J. Am. Chem. Soc.* **1968**, *90*, 4472-4473.
[10] R. J. H. Clark, T. J. Dines, L. T. H. Ferris, *J. Chem. Soc., Dalton Trans.* **1982**, 2237-2242.
[11] I. D. Brown, D. B. Crump, R. J. Gillespie, *Inorg. Chem.* **1971**, *10*, 2319-2323.
[12] G. Cardinal, R. J. Gillespie, J. F. Sawyer, J. E. Vekris, *J. Chem. Soc., Dalton Trans.* **1982**, 765-779.
[13] T. W. Couch, D. A. Lokken, J. D. Corbett, *Inorg. Chem.* **1972**, *11*, 357-362.
[14] R. Minkwitz, H. Borrmann, J. Nowicki, *Z. Naturforsch. B* **1991**, *46*, 629-634.
[15] R. C. Burns, R. J. Gillespie, W.-C. Luk, D. R. Slim, *Inorg. Chem.* **1979**, *18*, 3086-3094.
[16] J. Beck, K.-J. Schlitt, *Chem. Ber.* **1995**, *128*, 763-766.
[17] J. Beck, J. Wetterau, *Inorg. Chem.* **1995**, *34*, 6202-6204.
[18] J. Beck, *Angew. Chem. Int. Ed.* **2003**, *33*, 163-172.
[19] P. Boldrini, I. D. Brown, M. J. Collins, R. J. Gillespie, E. Maharajh, D. R. Slim, J. F. Sawyer, *Inorg. Chem.* **1985**, *24*, 4302-4307.
[20] R. C. Burns, M. J. Collins, S. M. Eicher, R. J. Gillespie, J. F. Sawyer, *Inorg. Chem.* **1988**, *27*, 1807-1813.
[21] M. J. Collins, R. J. Gillespie, J. F. Sawyer, *Inorg. Chem.* **1987**, *26*, 1476-1481.
[22] R. J. Gillespie, W. Luk, E. Maharajh, D. R. Slim, *Inorg. Chem.* **1977**, *16*, 892-896.
[23] J. D. Corbett, R. K. McMullan, D. J. Prince, *Inorg. Chem.* **1971**, *10*, 1749-1753.
[24] J. Beck, T. Hilbert, *Z. Anorg. Allg. Chem.* **2000**, *626*, 837-844.
[25] R. C. Burns, W.-L. Chan, R. J. Gillespie, W.-C. Luk, J. F. Sawyer, D. R. Slim, *Inorg. Chem.* **1980**, *19*, 1432-1439.
[26] C. Schulz, J. Daniels, T. Bredow, J. Beck, *Angew. Chem. Int. Ed.* **2016**, *55*, 1173-1177.
[27] T. Chivers, R. S. Laitinen, *Chem. Soc. Rev.* **2015**, *44*, 1725-1739.
[28] J. Beck, *Angew. Chem. Int. Ed.* **1994**, *33*, 163-172.
[29] R. C. Paul, C. L. Arora, J. K. Puri, R. N. Virmani, K. C. Malhotra, *J. Chem. Soc., Dalton Trans.* **1972**, 781-784.
[30] T. Zhang, T. Cai, W. Xing, T. Li, B. Liang, H. Hu, L. Zhao, X. Li, Z. Yan, *Energy Storage Mater.* **2021**, *41*, 667-676.
[31] R. Sun, H. Li, D. Zhang, D. Meng, C. Zhao, S. Jin, *J. Am. Chem. Soc.* **2025**, *147*, 24201-24205.

[32] E. Ahmed, J. Beck, J. Daniels, T. Doert, S. J. Eck, A. Heerwig, A. Isaeva, S. Lidin, M. Ruck, W. Schnelle, A. Stankowski, *Angew. Chem. Int. Ed.* **2012**, *51*, 8106-8109.
[33] D. J. Pascoe, K. B. Ling, S. L. Cockroft, *J. Am. Chem. Soc.* **2017**, *139*, 15160-15167.
[34] L. Vogel, P. Wonner, S. M. Huber, *Angew. Chem. Int. Ed.* **2019**, *58*, 1880-1891.
[35] A. Dhaka, I.-R. Jeon, M. Fourmigué, *Acc. Chem. Res.* **2024**, *57*, 362-374.
[36] P. Scilabra, G. Terraneo, G. Resnati, *Acc. Chem. Res.* **2019**, *52*, 1313-1324.
[37] S. Benz, J. López-Andarias, J. Mareda, N. Sakai, S. Matile, *Angew. Chem. Int. Ed.* **2017**, *56*, 812-815.
[38] P. Wonner, A. Dreger, L. Vogel, E. Engelage, S. M. Huber, *Angew. Chem. Int. Ed.* **2019**, *58*, 16923-16927.
[39] E. Chauhan, D. Giri, V. Govindaraj, G. Mugesh, *Angew. Chem.* **2025**, *137*, e202511786.
[40] S. Benz, M. Macchione, Q. Verolet, J. Mareda, N. Sakai, S. Matile, *J. Am. Chem. Soc.* **2016**, *138*, 9093-9096.
[41] A. Pizzi, A. Dhaka, R. Beccaria, G. Resnati, *Chem. Soc. Rev.* **2024**, *53*, 6654-6674.
[42] R. Gleiter, G. Haberhauer, D. B. Werz, F. Rominger, C. Bleiholder, *Chem. Rev.* **2018**, *118*, 2010-2041.
[43] E. Turgunbajew, M. Symeonidis, J. Langwald, L. Schumacher, H. A. Höppe, R. Pöttgen, J. Bruns, M. S. Wickleder, **2026**, *Unpublished work*.
[44] J. Langwald, L. Ebels, M. Symeonidis, J. Bruns, A. Frontera, M. S. Wickleder, **2026**, *unpublished work*.
[45] J. Barr, R. J. Gillespie, R. Kapoor, K. C. Malhotra, *Can. J. Chem.* **1968**, *46*, 149-159.
[46] R. J. Gillespie, J. Barr, G. P. Pez, P. Ummat, O. Vaidya, *Inorg. Chem.* **1971**, *10*, 362-367.
[47] C. Logemann, J. Bruns, L. V. Schindler, V. Zimmermann, M. S. Wickleder, *Z. Anorg. Allg. Chem.* **2015**, *641*, 831-837.
[48] K. Tanaka, T. Yamabe, H. Teramae, K. Fukui, *Inorg. Chem.* **1979**, *18*, 3591-3595.
[49] L. J. Saethre, O. Gropen, *Can. J. Chem.* **1992**, *70*, 348-352.
[50] D. van Gerven, S. Sutorius, J. Bruns, M. S. Wickleder, *ChemistryOpen* **2022**, *11*, e202200122.
[51] T. Steiner, *Angew. Chem. Int. Ed.* **2002**, *41*, 48-76.
[52] L. V. Schindler, M. Daub, M. Struckmann, A. Weiz, H. Hillebrecht, M. S. Wickleder, *Z. Anorg. Allg. Chem.* **2015**, *641*, 2604-2609.
[53] J. Langwald, R. M. Gomila, D. van Gerven, A. Frontera, M. S. Wickleder, *Dalton Trans.* **2025**, *54*, 16095-16105.
[54] L. V. Schindler, T. Klüner, M. S. Wickleder, *Chem. Eur. J.* **2016**, *22*, 13865-13870.
[55] J. Bruns, C. Kolb, M. S. Wickleder, *Z. Anorg. Allg. Chem.* **2014**, *640*, 2345.
[56] M. Zink, D. Thönnes, D. Ernsthäuser, J. Daniels, T. Bredow, J. Beck, *Z. Anorg. Allg. Chem.* **2024**, *650*, e202400112.
[57] M. A. Grasser, T. Pietsch, J. Blasius, O. Holloczki, E. Brunner, T. Doert, M. Ruck, *Chem. Eur. J. Chem Eur J* **2022**, *28*, e202103770.
[58] J. Beck, *Chem. Ber.* **1995**, *128*, 23-27.
[59] J. Beck, G. Bock, *Z. Anorg. Allg. Chem.* **1996**, *622*, 823-828.
[60] J. Beck, *Coord. Chem. Rev.* **1997**, *163*, 55-70.
[61] M. J. Collins, R. J. Gillespie, J. F. Sawyer, *Acta Cryst. Sect. C* **1988**, *44*, 405-409.
[62] P. D. Lyne, D. M. P. Mingos, T. Ziegler, *J. Chem. Soc., Dalton Trans.* **1992**, 2743-2747.
[63] V. Angarov, S. Kozuch, *New J. Chem.* **2018**, *42*, 1413-1422.
[64] R. Hein, P. D. Beer, *Chem. Sci.* **2022**, *13*, 7098-7125.
[65] A. Frontera, A. Bauza, in *Int. J. Mol. Sci., Vol. 22*, **2021**, p. 12550.
[66] A. Bauzá, D. Quinonero, P. M. Deya, A. Frontera, *CrystEngComm* **2013**, *15*, 3137-3144.
[67] J. S. Murray, G. Resnati, P. Politzer, *Faraday Discuss.* **2017**, *203*, 113-130.
[68] P. Politzer, J. S. Murray, T. Clark, G. Resnati, *Phys. Chem. Chem. Phys.* **2017**, *19*, 32166-32178.
[69] P. Politzer, J. S. Murray, *Crystals* **2019**, *9*, 165.
[70] I. Krossing, J. Passmore, *Inorg. Chem.* **1999**, *38*, 5203-5211.
[71] H. M. Tuononen, R. Suontamo, J. Valkonen, R. S. Laitinen, *J. Phys. Chem. A* **2004**, *108*, 5670-5677.
[72] S. Brownridge, I. Krossing, J. Passmore, H. D. B. Jenkins, H. K. Roobottom, *Coord. Chem. Rev.* **2000**, *197*, 397-481.
[73] J. Beck, G. Bock, *Angew. Chem. Int. Ed.* **1995**, *34*, 2559-2561.

[74] J. Beck, A. Fischer, A. Stankowski, *Z. Anorg. Allg. Chem.* **2002**, *628*, 2542-2548.
View Article Online
DOI: 10.1039/D6DT01115B

View Article Online
DOI: 10.1039/D6DT01115B

Data availability

The data supporting this article have been included as part of the supplementary information (SI). Supplementary information: including experimental details, synthesis, Raman spectra, X-ray powder diffraction, computational details, crystallographic information, and additional characterization data. See DOI: https:// doi.org/.

CCDC 2477856 (for $[Se_4][HS_2O_7]_2$), 2504489 (for $[Se_4][S_2O_7]$), 2476927 (for $[Se_4][HS_3O_{10}]_2$), 2476926 (for $[Te_4][HS_3O_{10}]_2$), 2476929 (for $[Te_6][HS_3O_{10}]_4$), 2476936 (for $[Te_6][HS_3O_{10}]_4$-II), 2502407 (for $[Te_6][S_4O_{13}]_2$), contain the supplementary crystallographic data for this paper.